VOL. 11, NO. 21, NOVEMBER 2016 ISSN 1819-6608
ARPN Journal of Engineering and Applied Sciences

www.arpnjournals.com

SATURATION AND PARABOLIC EFFECTS OF LANGLEY CALIBRATION AT DIFFERENT ALTITUDE LEVELS

Chang H. W. J.[1], Maizan N. H. N.[2], Chee F. P.[2], Sentian J.[3], Kong S. S. K.[3] and Dayou J.[2]
[1]Preparatory Center for Science and Technology, Universiti Malaysia Sabah, Jalan UMS, Kota Kinabalu, Sabah, Malaysia
[2]Energy, Vibration and Sound Research Group (e-VIBS), Faculty Science and Natural Resources, Universiti Malaysia Sabah, Jalan UMS, Kota Kinabalu, Sabah, Malaysia
[3]Climate Change Research Group (CCRG), Faculty Science and Natural Resources, Universiti Malaysia Sabah, Jalan UMS, Kota Kinabalu, Sabah, Malaysia
E-Mail: jacksonchw@ums.edu.my

ABSTRACT

The performance of the well-known Langley plot technique, used for the calibration of ground-based sunphotometers, has been investigated at three observatory sites of different altitudes. All solar measurements were collected using a portable LED-type sunphotometer programed to a constant measurement protocol to allow direct comparison between different days and sites. Our results show that evaluation on the correlation R-value and slope AOD-value alone is not robust enough to guarantee a good Langley plot. Statistical analysis on global, diffuse and direct component also fails to select a perfect Langley plot within a pool of data available. Instead, examination on the evolution of diffuse component and direct component against global component actually provides a good representation of the performance of Langley plot. Diurnal evolution of diffuse component and direct component was found closely matching to the global component in a similar increasing trend. Our results also highlighted two important effects that greatly govern the performance of Langley plot, which are saturation effect and parabolic effect. Saturation effect occurs for the state when little to no more signal increase can be legibly reflected on Langley plot. It is dominant in low airmass region where the change of airmass is relatively too small for the increase in signal detected by the sunphotometer. Parabolic effect is preceding effect of signal saturation and becomes severely erroneous when high air masses are included in Langley plot.

Keywords: airmass, langley plot, calibration, sunphotometer, solar.

1. INTRODUCTION

Sunphotometeric measurements are frequently used to understand the role of aerosol on the Earth's radiative budget [1]. However, error in the sunphotometeric calibration lead to artificial diurnal variation causes uncertainty in AOD retrieval [2]. There are two methods to calibrate ground based sunphotometer namely absolute method and Langley method. The absolute method uses a standard laboratory lamp illuminated on the instrument's sensor and the output voltage is calibrated against the spectrum of the lamp which is well known [3]. The absolute method of calibration is difficult and requires a good knowledge of the bandpass response of each channel and several precise measurements. Besides, the precision lamp accuracy is not easy to maintain and it must be recalibrated regularly [4]. Most of the difficulties of absolute method are bypassed by the Langley method where it eliminates the need for band pass integration, a standard lamp, necessary power supplies and high-end accessories such as integrating sphere [5].

A good Langley plot requires a perfectly clear and cloud free sunset or sunrise. The idea behind this is having enough variation in the atmospheric air mass while the optical depth remains constant. For this purpose, air mass range from 2 to 6 is usually used in common Langley method. Lower air mass is avoided because it tends to have slower rate of change [6] and higher air mass always possess high uncertainty due to increase in atmospheric temperature [7]. Besides, another important requirement for a good Langley plot is the aerosol loading to be kept as constant as possible during the entire interval [8]. In most cases, constant aerosol loading across wide range of air mass is nearly implausible. The closest way to achieve such condition is to perform the Langley measurement at high altitude where low atmospheric optical depth and stable aerosol loading is highly to be expected [9]. Atmospheric transmittance is a function of the attenuation of extraterrestrial irradiance by scattering and absorption [10]. Measurement of direct irradiance at specific wavelength by ground based sunphotometer is expressed by Lambert- Beer laws as [11]:

$$\ln P_\lambda = \ln P_{o,\lambda} - \sum \tau_{\lambda,I} m_i \quad (1)$$

where P_λ is solar intensity at wavelength λ on the surface, $P_{o,\lambda}$ is solar intensity at wavelength λ outside the atmosphere, m_i isopticalairmass, $\tau_{\lambda,I}$ istotal optical depth at wavelength λ of the atmosphere. From the Eq. (1), $\ln P_\lambda$ is linearly related to m as long as $\tau_{\lambda,I}$ is constant during the measurement period. The extraterrestrial constant of $P_{o,\lambda}$ can be estimated by extrapolating the straight line on the Langey plots directly to zero air mass [12]. As the atmospheric stability is required, measurement site for Langley calibration is very limited. Big cities and industrial area are obviously evaded. High altitude and clean area such as Mauna Loa, Hawaii are preferred location for Langley measurement. Turbid sites are often inhibited by unstable atmospheric condition due

to trapping of aerosol inside the marine inversion later which usually broken through upslope winds [13].

In this paper, the performance of the conventional Langley calibration measured at three different altitude levels was investigated. We present data on the consistency and reliability of measurements achieved with a portable LED-type sunphotometer. The work focuses on an initial characterization study on the Langley plot measured at different altitude levels. We discuss the evaluation method to select appropriate dataset suitable for Langley plot when the daily sky condition is unknown. Initial results suggest that diurnal evolution of direct and diffuse component against global component is an effective parameter useful for sky condition representation. Besides, our results also highlighted two important effects that greatly govern the performance of Langley plot. Details of these effects are discussed in this paper.

2. DATA AND INSTRUMENTATION

In this work, Langley measurement was performed at three observatory sites. The details of these three observatory sites are depicted in Table-1. The observations were categorized into Site A for high altitude at 3,800 m a.s.l., Site B for mid altitude (1,500 m a.s.l.), and Site C for low altitude (7 m a.s.l.). All sites have the same geospatial coordinate approximately at 5.98°N, 116.07°E which is located at Kota Kinabalu. The city of Kota Kinabalu (latitude 5.9804° N, longitude 116.0735° E) is located at northwest coast of Borneo facing the South China Sea. It is the gateway to Mount Kinabalu (4,095 m a.s.l.), which is situated about 50 kilometres east-northeast of the city. As part of Sabah area, Kota Kinabalu features a typical equatorial climate with constant temperature and considerable amount of rain and high humidity. The climate of the city experiences two prevailing monsoons the Northeast Monsoon and the Southwest Monsoon. The Northeast Monsoon occurs between November and March, while the Southwest Monsoon occurs between May and September. There are also two successive inter-monsoons from April to May and from September to October. On average, Kota Kinabalu's temperature ranges from 26°C to 28°C where April and May (average high temp. ~32°C) are the hottest months and January (average high temp. ~30°C) is the coolest month. The average annual rainfall is around 2,400 mm and varies throughout the year with February and March are typically the driest months and rainfall peaks in the inter-monsoon period in October. All solar measurements were made using a portable LED-type sunphotometer. It uses a charged-couple device (CCD) as detector to measure light signal against wavelength in the range 300 nm to 1000 nm. Signal was measured in voltage read by the CCD and converted into counts in pixels. Exposure time was set at 10 ms and each measured data point was averaged with 5 scans. This measurement protocol was set constant for all three sites Langley measurement.

Table-1. Details of Langley measurement at each observatory sites.

Site	Site A (High)	Site B (Mid)	Site C (Low)
Altitude	3,270 m a.s.l.	1,574 m a.s.l.	18 m a.s.l.
Location	Laban Rata	Kinabalu Park	Sepanggar, UMS
Coordinate	6.05 °N, 116.56°E	6.00°N, 116.54°E	6.03°N, 116.12°E
Measurement Date (dd-mm-yy)	22/1/16- 27/1/16	26/8/15- 30/8/15	13/1/16-2/3/16
Measurement Period (hrs)	2~3	2~3	2~3
Measurement Interval (min)	3	3	3
Air mass range	1-8	1-6	1-4
Solar Zenith Angle (deg)	46- 86	42- 80	40- 77

3. RESULTS AND DISCUSSIONS

In this work, a total of 15 days Langley plot were collected for the three observatory sites at low, mid and high altitude levels. The measured signals in pixels were plotted against airmass for each observation day. Regression line is best fitted in linear form where the slope represents total aerosol optical depth and y-intercept represents the AM0 extrapolated value. Details of the regression Langley plot are depicted in Table-2. All Langley plots at low altitude sites exhibit high correlation of R^2>0.8. Meanwhile for mid and high altitude sites, the correlation R-value is not consistent for all days but rather random in the range 0.2~0.9, depending on the performance of the Langley dataset itself. Expected pattern of increasing Langley correlation R-value for decreasing slope-value was not consistently observed. Instead, this association was found poorly correlated. Low slope-value does not necessarily produce high correlation R-value. The highest R-value (R^2=0.93) was observed on Day 5 at low altitude with considerably high AOD-value equals to 0.57, while the lowest R-value (R^2=0.18) was observed on Day 14 at high altitude with slightly similar AOD-value at 0.53. Also, the highest and lowest AOD-value was neither remarked on the poorest and best Langley plot, respectively (see Day 10 at mid altitude and Day 13 at high altitude in Table 2). This indicates that evaluation on the Langley correlation R-value and slope-value alone is not robust enough to guarantee a perfect

Langley plot. Langley correlation R-value and slope AOD-value are merely rough estimation of the performance of Langley plot. For even more severe cases, fictitious Langley plot is probable at some extends. For example, Day 10 at mid altitude, the day was complicated by heavy aerosol loading at AOD = 2.4 but yet having correlation R-value of 0.6.

Table-2. Daily Langley plot at 500nm for three observatory sites of different altitude levels. Regression line is best fitted in linear form y = a + bx where a represents the AM0 extrapolated value (Po) and b represents the aerosol optical depth (AOD), n is the total data points.

Low Altitude	**Day 1**	**Day 2**	**Day 3**	**Day 4**	**Day 5**
Regression line	y=-0.4106x+10.403	y=-0.3443x+10.215	y=-0.6684x+10.58	y=-0.438x+10.279	y=-0.5695x+10.575
Correlation coefficient	0.8717	0.9065	0.8232	0.836	0.9351
AOD (avg)	0.4106	0.3443	0.6684	0.438	0.5695
Po	0.649	2.445	1.041	1.834	0.993
n	41	36	39	51	39
Mid Altitude	**Day 6**	**Day 7**	**Day 8**	**Day 9**	**Day 10**
Regression line	y=-1.0175x+10.367	y=-0.2454x+10.198	y=-0.453x+10.533	y=-0.6648x+10.424	y=-2.3596x+13.669
Correlation coefficient	0.6204	0.881	0.6719	0.4151	0.5635
AOD (avg)	1.0175	0.2454	0.453	0.6648	2.3596
Po	10.367	10.198	10.533	10.424	13.669
n	40	46	50	44	37
High Altitude	**Day 11**	**Day 12**	**Day 13**	**Day 14**	**Day 15**
Regression line	y=-0.2889x+10.471	y=-0.9347x+11.178	y=-0.1899x+9.9723	y=-0.525x+9.5511	y=-0.259x+10.382
Correlation coefficient	0.7898	0.5514	0.4371	0.1847	0.7575
AOD (avg)	0.2889	0.9347	0.1899	0.525	0.259
Po	10.471	11.178	9.9723	9.5511	10.382
n	47	26	46	44	48

Table-3 shows the statistical analysis of signal reading in pixels for three components of solar insolation at wavelength 500 nm, namely global component (GC), diffuse component (DifC), and direct component (DirC). Global component is the total solar insolation measured by the instrument's sensor in direct pointing to the sun. Diffuse component is the solar insolation measured by the sensor after shading the sensor from direct pointing to the sun. Direct component is the subtraction of global component from diffuse component at distinct air mass. Under cloudless and homogenous sky condition, total solar insolation perceived at Earth surface is directly proportional to the altitude of the observatory site. For this comparison, we selected three discrete days at each altitude sites with the highest GC. Our results have the similar pattern showing higher altitude measures relatively higher maximum GC than that of lower altitude. Maximum GC measured at high altitude was Day 12 (17490), followed by mid altitude on Day 7 (16309), and low altitude on Day 4 (15867). Similar pattern was also observed for mean ± standard deviation of GC where Day 12 measured the highest mean value at 16032 ± 3077, followed by Day 7 (13464 ± 3219), and Day 3 (10009 ± 4723). When considering GC as the only indicator for evaluation, false interpretation is likely to occur. At many instances, high GC measured on a day could be due to the abundant contributions from DifC. One such example we highlighted in our results was Day 12 which measured the highest GC amongst all days, but also having high avg. ± std. dev. on DifC for 3683 ± 955. High DifC are basically results from heavy scattering of solar insolation by various constituents in air. This scattering is caused by random particles in air such as aerosols or cloud cover that occur within the short intervals during the Langley measurement. Hence, days with high DifC are technically assumed as aerosol-polluted or cloudy days. Therefore, evaluation on Langley plot performance using GC seems contradicting and misleading at some circumstances.

Table-3. Statistical analysis of signal reading in pixels for global component (GC), diffuse component (DifC), and direct component (DirC) at wavelength 500 nm within daily Langley measurement at three observatory sites of different altitude levels.

Low Altitude	**Signal** (Pixels)	**Day 1**	**Day 2**	**Day 3**	**Day 4**	**Day 5**
Global Component (GC)	mean ± stddev	12235 ± 3395	12394 ± 2783	10009 ± 4723	12195 ± 3437	10978 ± 3778
	min, max	4091, 15423	6268, 15489	1879, 15674	3179, 15867	3081, 15189
	Range	11332	9221	13796	12688	12108
Diffuse Component (DifC)	mean ± stddev	2979 ± 538	3153 ± 474	2797 ± 737	2803 ± 745	2610 ± 572
	min, max	1657, 3518	2034, 3594	1286, 3701	1420, 4643	1366, 3273
	Range	1862	1560	2415	3223	1907
Direct Component (DirC)	mean ± stddev	9226 ± 2917	9241 ± 2326	7213 ± 4115	9392 ± 2888	8359 ± 3216
	min, max	2301, 11981	4234, 11953	20, 12358	1759, 12076	1678, 11953
	Range	9679	7719	12338	10317	10274
n		41	36	39	51	39
Mid Altitude	**Signal** (Pixels)	**Day 6**	**Day 7**	**Day 8**	**Day 9**	**Day 10**
Global Component (GC)	mean ± stddev	8201 ± 3063	13464 ± 3219	11764 ± 4059	9398 ± 4380	11803 ± 4888
	min, max	1993, 12097	5654, 16309	1072, 15986	1310, 15221	1202, 15898
	range	10104	10655	14914	13911	14696
Diffuse Component (DifC)	mean ± stddev	4290 ± 1398	1392 ± 243	1405 ± 679	2376 ± 928	1917 ± 694
	min, max	1786, 6446	911, 2112	815, 5999	1031, 5521	1118, 5790
	range	4660	1201	5184	4491	4672
Direct Component (DirC)	mean ± stddev	3910 ± 2029	12073 ± 3010	10359 ± 3943	7023 ± 3968	9886 ± 4780
	min, max	206, 7045	4742, 14773	257, 14457	14, 12859	2, 13548
	range	6839	10031	14199	12844	13546
n		40	46	50	44	37
High Altitude	**Signal** (Pixels)	**Day 11**	**Day 12**	**Day 13**	**Day 14**	**Day 15**
Global Component (GC)	mean ± stddev	13382 ± 4529	16032 ± 3077	12106 ± 4594	9119 ± 4705	13545 ± 4338
	min, max	1518, 16954	6576, 17490	656, 17148	732, 17343	1390, 16919
	range	15435	10914	16493	16612	15529
Diffuse Component (DifC)	mean ± stddev	1866 ± 400	3683 ± 955	3399 ± 2099	4340 ± 2553	1843 ± 451
	min, max	812, 2235	742, 5268	639, 14400	659, 8238	805, 2443
	range	1423	4525	13761	7579	1638
Direct Component (DirC)	mean ± stddev	11516 ± 4131	12349 ± 2730	9208 ± 3639	4789 ± 4044	11699 ± 3913
	min, max	687, 14828	4566, 14111	17, 13655	41, 11778	585, 14880
	range	14140	9544	13638	11736	14295
n		47	26	46	44	48

On average, observation on DirCstatistic is similar to that of GC where higher altitude measures higher DirC and decreases for lower altitude. Three nominal days with the highest DirC at each altitude site were selected for comparison. At high altitude, Day 15 measured the highest max DirC at 14880 (11699 ± 3913), followed by mid altitude Day 7 at 14773 (12073 ± 3010), and low altitude Day 3 at 12358 (7213 ± 4115). In the same way, DirC also has the potential of misleading to falsification of Langley plot performance evaluation. Similarly, we highlight this contradiction on Day 12 which measured the highest DirC at 12349 ± 2730 (max. 14111) amongst all other days, but yet having high DifC that indicates the high likeliness of the day heavily polluted by aerosol and cloud cover. We explain this contradiction as preceding misinterpretation because DirC is merely subtraction of GC from the corresponding DifC at distinct airmass.

On the other hand, statistical analysis on DifC is different from both GC and DirC. Min DifC from high altitude were mostly lower than that of mid and low altitudes. The lowest min DifC was measured on Day 13 from high altitude at 639, followed by Day 8 from mid altitude at 815, and Day 3 from low altitude at 1286. On average, Day 7 from mid altitude has the lowest DifC mean value and least deviation at 1392 ± 243, followed by Day 8 of the same altitude at 1405 ± 679. For high altitude sites, Day 11 and 15 both measured quite low and stable DifC at 1866 ± 400 and 1843 ± 451, respectively. In terms of range (max – min), Day 7 at mid altitude remarks the least range at 1201, followed by Day 11 at high altitude (1423), and Day 15 (1638). However, the range for Day 8 was considerably high at 5184. High range of DifC possibly implies the contamination of the dataset by short intervals of thin cirrus clouds but offsets by the averaging factor. Two possible assumptions could be made to explain this outlier, one being the systematic errors from the instrument itself and the other being the very short intervals of thin cirrus clouds occurred during the measurement.

Figure-1 shows the boxplot of GC, DifC, and DirC on each observation day at three different altitude levels. Examination on the boxplot further reveals the robustness of DifC in evaluating the cloudiness of the sky condition within the Langley measurement. At low altitude, DifC disperses the most on Day 4 with the standard deviation ±745, followed by mid altitude on Day 6 (±1398), and high altitude on Day 14 (±2553). Statistically, they contained many values considerably deviated from the mean value. It reflects these days are high likely contaminated by random intervals of thin cirrus clouds or heavy cloud loadings within the measurement. On DirC boxplot, data that falls out from the normal distribution are represented by circles. These extreme points are too subjective to be used as indicator of the performance of Langley plot. It is hardly to perfectly remove these outliers even for days that considered clear sky. For example, Day 11 that have low and quite stable DifC, contained outliers during the early intervals measurement. We have no intention to justify these points are contaminated by clouds or heavy aerosols, mainly because they were measured in the high airmass region which genuinely should be expected low in solar signal reading. However, one thing that can be confirmed is the deviation of DifC greatly reflects the performance of Langley plot. For a given observation day that has low deviation on DifC, the day is high likely suitable for further use in Langley plot. Examples were shown by Day 2 (low altitude), Day 7 (mid altitude), and Day 11 (high altitude).

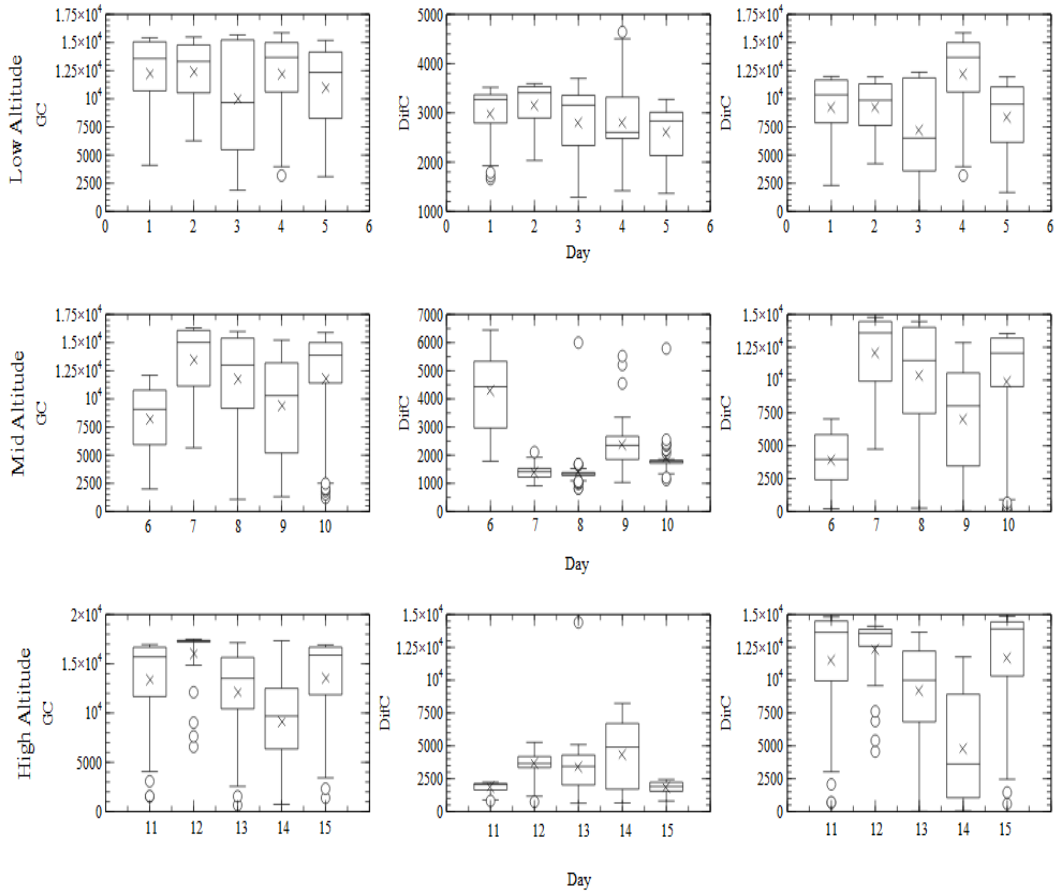

Figure-1. Boxplot of global component, diffuse component and direct component for low altitude (upper), mid altitude (middle) and high altitude (lower) on daily basis. Day 1 to 5 at low altitude, Day 6 to 10 at mid altitude, Day 11 to 15 at high altitude.

We shortlisted three days with nearly perfect increasing pattern between DirC and GC to further examine the characteristics of Langley plot obtained on these days. The shortlisted days are Day 2, 7, and 11 which are representative of low, mid and high altitude, respectively. Figure-2 shows the Langley plot for the three selected days. In the mid airmass region, higher altitude site consistently measures greater signal lnP at distinct airmass. It can be explained by the fact that longer optical path length travelled by the sunlight basically increases the likeliness of the direct component solar insolation scattered by random particles presented in air. Therefore, low altitude site measured lower signal ln P than mid altitude and subsequently followed by high altitude at the same airmass. However, when it comes close to low airmass region where the intensity of sunlight is the most intense, measured signal ln P started to saturate and gives values of almost same readings. The saturation is more dominant for measurements taken at high and mid altitude site. For high altitude measurement, airmass beyond 3.0rise of the signal reading was too little to significantly affect the Langley regression. Similar characteristics was also observed for mid altitude measurement where saturation of signal ln P readings started beyond airmass 2.0. This effect severely inhibits the Langley extrapolation to yield a robust regression line of high correlation R-value. Nonetheless, the saturation effect was not observed for measurements taken at low altitude. One can see from Figure-2 that a nearly perfect increasing ln P matches the decreasing airmass from 4 to 2 on Day 2 of low altitude. The signal saturation occurs in the low airmass region is due to the fact that the change of airmass is relatively too small for the little increase in solar signal reading.

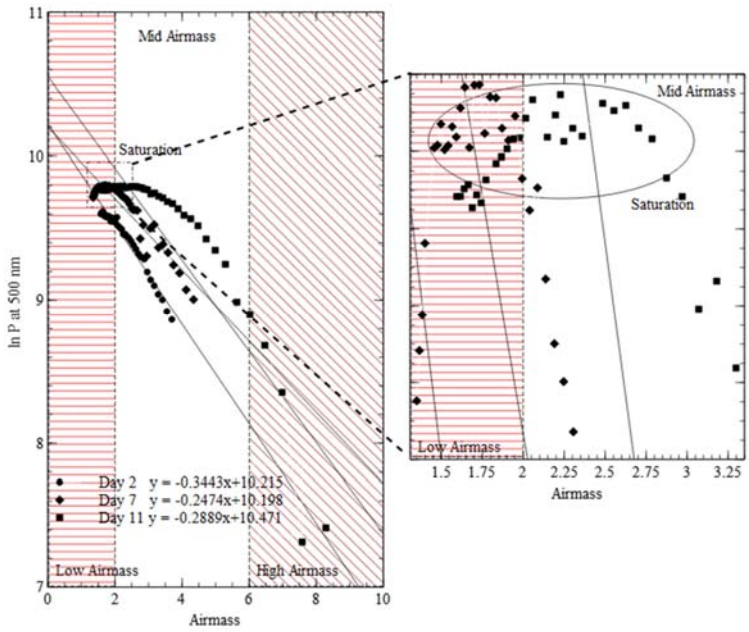

Figure-2. Saturation effect on Langley plot for Day 7 at mid altitude, and Day 11 at high altitude.

The preceding effect from signal saturation in low airmass region was catalyst to the parabolic effect occurred at high and mid altitude measurement. Figure-3(a) demonstrates the parabolic effect on Day 7 and 11. Both Langley plots were complicated by saturation of ln P signal particularly for airmass close to low AMregion. The resulting saturation effect bends the Langley plot into a parabolic-like curve. An even more erroneous parabolic curve was yielded when data from high airmass further bends the curve into quadratic-like (see best fitted curve line on Day 11 on Figure-3(a)). To correct the saturation and parabolic effects, we restricted the airmass range for mid and high altitude Langley plot nominally. Figure-3(b) shows the Langley plot of the restricted airmass range for Day 7 and Day 11. After the restriction, the resultant Langley plot remarks significant improvement on correlation R-value of greater than 0.94. A more realistic result on the Langley extrapolated value was also observable where mid altitude extrapolates to 10.44 and high altitude extrapolates to 10.71. Table-4 summarizes the details of the Langley plot before and after restriction on the three selected days. On average, Langley calibration at lower altitude levels is expected to produce a lower AM0 extrapolated value under cloudless sky condition. From the result findings, the extrapolated value at low altitude level is underestimated by 4.6% and mid altitude level by 2.5%. The findings also highlighted the important of airmass range selection for high and mid Langley measurements. Stricter airmass range should be carefully constrained for better correlation R-value Langley regression. When this effect could be insignificant for low altitude Langley measurement, but its effect on mid and high altitude measurement is essential crucial to consider. Neglecting the suitable airmass range is likely to fictitiously yield inaccurate or impractical Langley plot which leads to erroneous AM0 extrapolated value.

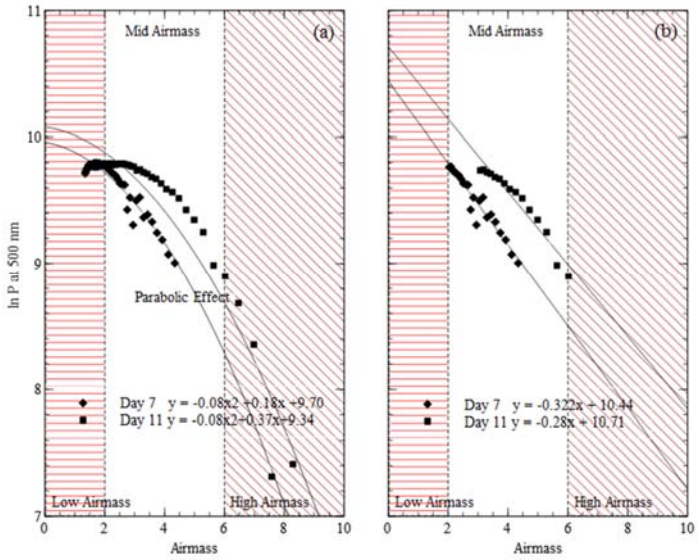

Figure-3. Langley plot (a) parabolic effects of unsuitable airmass range (b) restricted airmass range on Day 7 and 11 for mid and high altitude.

Table-4. Summary of AM0 Langley extrapolation before and after airmass restriction for the three selected Langley days.

	Before AM restriction			**After AM restriction**		
Day	**Day 2**	**Day 7**	**Day 11**	**Day 2**	**Day 7**	**Day 11**
Regression	y=-0.3443x+10.215	y=-0.2454x+10.198	y=-0.2889x+10.471	y=-0.3443x+10.215	y=-0.3221x+10.44	y=-0.2831x+10.71
R-value	0.9065	0.881	0.7898	0.9065	0.9401	0.9405
Airmass	1.5~4.5	1.5~4.0	1.5~8.0	1.5~4.5	2.0~4.0	3.0~6.0
AM range	3.0	3.5	6.5	3.0	2.0	3.0
AOD (avg)	0.3443	0.2454	0.2889	0.3443	0.3221	0.2831
Po	10.215	10.198	10.471	10.215	10.441	10.710
n	36	46	47	36	23	15

4. CONCLUSIONS

In this work, a total 15 Langley days were collected using a portable LED-type sunphotometer at three observatory sites of different altitudes. The measured signal ln P was plotted against airmass to produce Langley plot for each observation day. The Langley correlation R-value and slope AOD-value were not consistent from day to day and rather random depending on the performance of dataset itself. Statistical analysis on the global, diffuse and direct component was also clueless to accurately determine the perfect Langley plot for a given pool of data available. Our results suggested that when plotting the direct component against the global component in time-series evolution, a highly linear relationship is likely to observe for good Langley plot. Under ideal sky condition for Langley measurement, the increase between direct component and global component are correlated in a perfectly linear form due to the decreasing optical path length in airmass. For the same reason, similar trend was also observed for diurnal evolution between diffuse component and global component, but the trend strength was not as strong as that of direct component. This characteristic is useful indicator to accurately characterize a good Langley plot with better confidence.

Our results also highlighted two important effects that greatly govern the robustness of Langley plot. The first is the saturation effect which occurs mostly in the low airmass region. This effect is more dominant for high and mid altitude measurement. At low altitude site, the intensity of solar signal was not intense and therefore the saturation effect was not significantly observable. Meanwhile at mid and high altitude sites, higher solar intensity are likely expected for lower optical path length. On top of that, the change of airmass in low airmass region is relatively too small for the increase in solar signal. The overall consequence is therefore the signal saturated in the low airmass region especially for measurement taken at higher altitude sites. The second is the parabolic effect which occurs from the preceding effect of signal saturation in low airmass region and

become severely erroneous when high airmasses are included in Langley plot. The signal saturation in low airmass region bends the linear regression line into a curve line for decreasing airmass in Langley plot. The fictitious data from high airmasses further bends the curve line into quadratic-like curve.This effect was signified at high altitude because solar measurement was considerably possible even in high airmass regions for which the solar signal reading is still too low at low altitude.

ACKNOWLEDGEMENT

This research was supported by the Malaysian Ministry of Education under the research grant number RAG0071-SG-2015, and is greatly acknowledged.

REFERENCES

[1] Vladutescu D.V., Madhavan B.L., Gross B.M., Aguirre A., Moshary F., Ahmed S.A., Razani M., Blake R. A.2014. Assessment of Langley and NASA-GISS calibration techniques for mfrsr aerosol retrieval. IEEE Transactions on Geoscience and Remote Sensing. 52(9): 5880-5894.

[2] Moorthy K.K., Babu S.S., Satheesh S.K. 2003. Aerosol spectral optical depths over the Bay of Bengal: Role of transport. Geophysical Research Letters. 30(5):1-4.

[3] Parr A.C. 2001. The candela and photometric and radiometric measurements. Journal of Research of the National Institute of Standards and Technology. 106(1): 151- 186.

[4] Rutgers G.A.W. 1972. Absolute spectroradiometric measurements. Journal of Research of the National Bureau of Standards- A Physics and Chemistry. 76A (5): 427- 436.

[5] Slusser J., Gibson J., David B., Kolinski D., Disterhoft P., Lantz K., Beaubien A. 2000.Langley method for calibrating UV filter radiometer. Journal of Geophysical Research.10: 4841-4849.

[6] Kiedron P.W., Michalsky J.J. 2016. Non-parametric and least squares Langley plot methods. Atmospheric Measurement Techniques. 9: 215-225.

[7] Chang J.H.W, Dayou J., Sentian J. 2014. Development of near-sea-level calibration algorithm for aerosol optical depth measurement using ground-based spectrometer. Aerosol and Air Quality Research.14 (1): 380-395.

[8] Silva A.A. 2006. Calmness of the aerosol layer in the atmosphere during biomass burning episodes. Journal of Geophysical Research Atmosphere. 111(D11): 1-11.

[9] Kreuter A., Wuttke S., Blumthaler M. 2013. Improving Langley Calibrations by reducing diurnal variations of aerosol Angstrom parameters. Atmospheric Measurement Technique. 6: 99-103.

[10] Bayat A., Masoumi A., Khalesifard H.R. 2011.Retrieval of atmospheric optical parameters from ground-based sun-photometer measurements for Zanjan, Iran. Atmospheric Measurement Technique. 4: 457-463.

[11] Pawar G.V., Devara P.C.S., More S.D., Kumar P.P., Aher G.R. 2012. Determination of aerosol characteristics and direct radiative forcing at Pune. Aerosol and Air Quality Research.12: 1166- 1180.

[12] Kobayashi T. 1981. The design of a new sunphotometer and some considerations on Langley calibration. Paper in Metereology and Geophysics. 32(2): 79-88.

[13] Wen G., Cahalan R. F., Holben B. N. 2003. Limitations of ground-based solar irradiance estimates due to atmospheric variations. Journal of Geophysical Research Atmosphere. 108(D14): 1-9.